

Aerosol Particle Spreading in an Operation Room under Dynamic Condition

Daniel Schmeling^{1}, Tobias Dehne¹, André Volkmann¹, Clemens Bulitta², Sebastian Buhl², Andreas Melzer^{3,4} and Axel Müller⁵*

¹ German Aerospace Center (DLR), Institute of Aerodynamics and Flow Technology, Department Ground Vehicles, Bunsenstr. 10, 37073 Göttingen, Germany

² Technical University of Applied Sciences Amberg-Weiden, Institute of Medical Technology, Hetzenrichter Weg 15, 92637 Weiden, Germany

³ University Leipzig, Faculty of Medicine, Semmelweisstraße 14, 04103 Leipzig, Germany

⁴ University Dundee, Institute for Medical Science & Technology, Dow Street, DD1 5HL Dundee, Scotland, UK

⁵ OHB Systems AG, Manfred-Fuchs-Str. 1, 82234 Wessling, Germany

Abstract. We report on the experimental investigation of aerosol particle spreading in an operation room. Different configurations regarding the source position or representative movements of the staff in the room are analyzed. The data acquisition is performed using a sensor grid of more than 50 particulate matter sensors at a measurement frequency of approximately 1 Hz operated with the DLR's mobile measurement system (MMS): This allows for a reasonable resolution in space and time. The measurement campaign was performed within the framework of the c3vis project in the teaching operational room of the OTH Amberg-Weiden. First results showed that the aerosol particles exhaled by the standing source are down-washed by the airflow and reach, strongly diluted, one of the sensor positions above the operation table next to the standing source. Local concentrations as low as $\approx 1.5\%$ of the exhalation concentration are found. All other positions above the operation table show a particle concentration close to zero. With a certain time delay the cloud of exhaled aerosol particles reaches single other sensor locations on its way towards the exhaust openings, while being further diluted ($\approx 0.03\%$ of the exhalation concentration). During the dynamic case, we found neglectable effects when the doors were opened or closed, a weak effect caused by the movement of the staff through the room and a strong effect on the aerosol concentration above the operation table when the surgeon was operating on the patient.

1 Introduction

Ventilation in operation rooms (ORs) is a critical component when it comes to maintaining a sterile environment and to avoid cross-contamination. The design and implementation of effective ventilation systems in ORs are subject to rigorous standards and recommendation guidelines stipulated by authoritative sources in the field of healthcare facility design. Organizations such as the American Society of Heating, Refrigerating and Air-Conditioning Engineers (ASHRAE) and the Centers for Disease Control and Prevention (CDC) offer guidelines that emphasize the importance of achieving optimal air exchange rates, filtration efficiency, and air cleanliness in ORs. The ventilation systems typically incorporate high-efficiency particulate air (HEPA) filters to remove micro-organisms and airborne particles.

Thus, high effort is invested to avoid particle transport from the patient's wound to present staff and vice versa by well-guided airflow from the ceiling to exhaust openings at floor level [1] – similar to the ventilation of clean rooms well known from, e.g., space industry during the assembly of optical measurement systems.

For a better comparison and to ensure sufficient air quality, many different standards are available worldwide. Some of these are summarized and compared in a review article by Melhado [2].

In general, most studies aim at assessing the ventilation quality in operation rooms addressing the relationship between operating room ventilation systems and surgical site infections (SSIs). In this context, the critical role of ventilation is to maintain a sterile environment is commonly emphasized. In specific, the different research groups discuss, e.g., the impact of air exchange rates, filtration methods, and airflow patterns on reducing microbial contamination and the subsequent risk of SSIs [3-7].

Most studies in the literature focus on static scenarios without any movement of the staff in the OR. However, it is well-known that the movement of persons influence the airflow and thus also increases the potential particle transport by the airflow. As an example, the study of Wood [8] is cited, who analyzed the transport of contaminants by walking persons in the ward of a hospital. Additionally, the staff in the OR may disturb the well-designed vertical airflow by, e.g., leaning over

* Corresponding author: daniel.schmeling@dlr.de

the patient to perform specific operation procedures. Such a dynamic bending process of the surgeon was analyzed by Chow and Wang [9] in a computational fluid dynamics analysis with generic persons in the OR. They found that when all surgical staff stands upright without moving, the ventilation system can keep the concentration of bacteria-carrying particles (BCPs) to less than 1 cfu/m^3 within the surgical critical zone. But in the scenario considering the periodic bending, the movement of a surgeon can cause the concentration of BCPs within the surgical critical zone to exceed the recommended 10 cfu/m^3 .

As there are still very few scientific studies on the effect of the movement, we address this point in the present manuscript. First of all, we have investigated different static postures of the surgeon and secondly, we have experimentally measured the local aerosol particle concentrations for a dynamic scenario where one assistant left the OR, re-entered with some surgery instruments, handed them to the surgeon who then started to move with the instruments. Furthermore, all measurements have been performed in a realistic environment with a heat-releasing patient manikin, real humans acting in the OR, performing typical motions as taught in medical education.

2 Experimental Setup and Methods

The measurement campaign was performed within the framework of the c3vis project in the teaching operational room of the OTH Amberg-Weiden [10]. Details on the room including the installed ventilation system and the installed measurement systems as well as the investigated parameter combinations are presented in this section.

2.1 Operation Room

The operation room, or operation room where the measurements were performed is an original and fully equipped room used for the medical education at the OTH Amberg-Weiden, see Fig. 1. It is equipped with a state-of-the-art ceiling-based air supply system consisting of 30 half-spheres to provide a low-momentum high-efficiency particulate air (HEPA) filtered clean air supply. 22 of these supply air openings are positioned in two circles directly above the operation table and provide a volume flow rate of $6450 \text{ m}^3/\text{h}$. The other 8 supply air openings are distributed over the rest of the ceiling and generate an additional volume flow of $2500 \text{ m}^3/\text{h}$. The exhaust air openings are located in the lower sidewalls 0.25 m above the floor close to the four corners of the room. The installed system ensures a well-guided downward-oriented airflow in an inner region in the operation room with the operation table in its center, see also [11, 12]. The dimensions of the room amount to approximately $7.75 \text{ m} \times 5.70 \text{ m} \times 2.75 \text{ m}$ (L x W x H). The operation room is connected via an automatic sliding door to the adjacent preparation room.

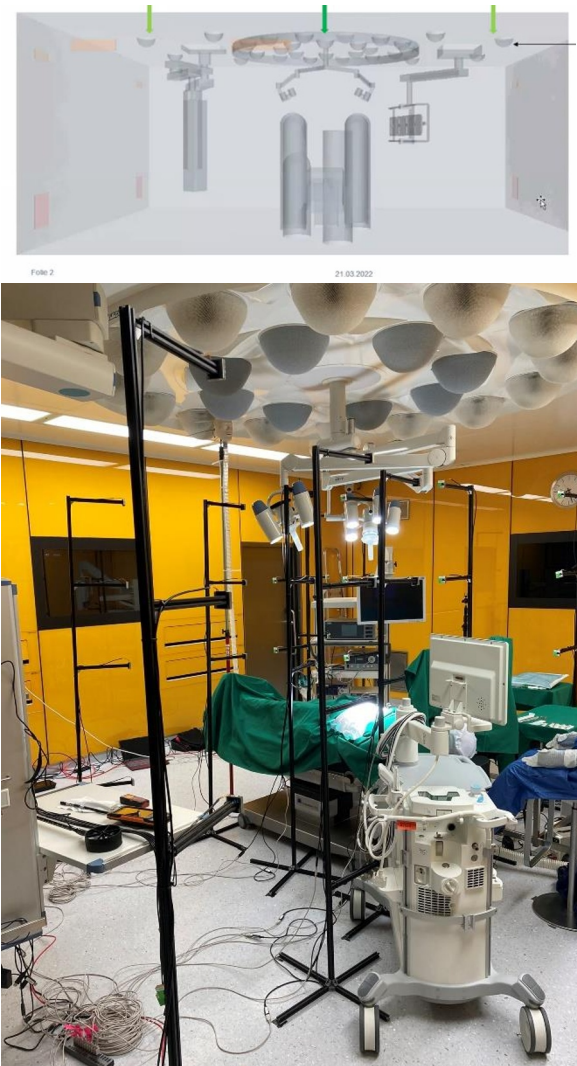


Fig. 1. Sketch of the operation room (top) and image of the operation room equipped with local sensor racks.

During the measurements we used a thermal manikin to simulate the patient and real humans as surgeon and staff. An infrared image of a typical scenario, i.e. the simulation of a regular laparoscopic procedure, during the measurements is shown in Fig. 2. The red areas reflect the warm heads and hands of the staff as well as the uncovered abdomen of the patient. The blue vertical and horizontal struts are the holding tripods of the particulate matter sensors, which are also visible in Fig. 1 and which are described in the following section.

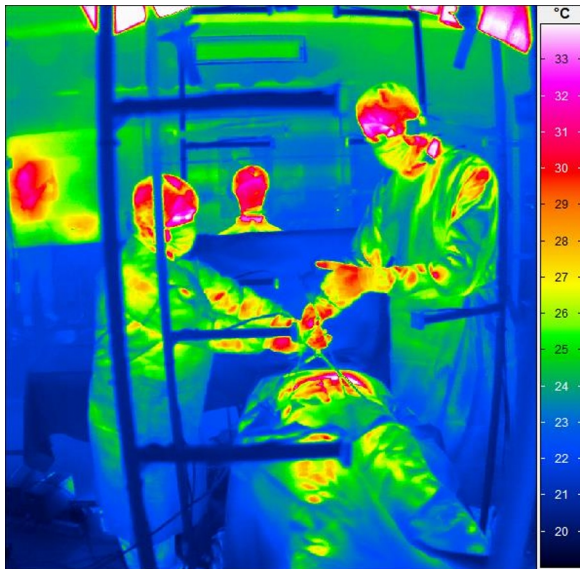


Fig. 2. Infrared thermography of the patient and the operating staff.

2.2 Particle Generation and Detection

The experimental analysis of the aerosol spreading comprises the generation of the aerosol particles and the local detection of the aerosol particle concentrations (for details see Schmeling et al. [13]). This measurement system has already been successfully applied in aircraft cabins [13] and train compartments [14].

2.2.1 Aerosol Generation

The aerosol generator consists of an airbrush pistol used to disperse a constant mist of artificial saliva (mixed in accordance with NRF 7.5, receipt see [Schmeling]). After the initial generation, the particles are guided through a settling chamber. The setup is designed in such way that the particles already have an age of more than one minute before being released into the room, i.e., all evaporation processes are expected to be finished, and pure dry particles are released. The particle size distribution of the generated particles shows that particles with diameters in the range between $0.3\ \mu\text{m}$ and $2.5\ \mu\text{m}$ are produced covering the range of particle sizes produced during normal breathing, for example. It should be noted that much more particles are released compared to a normally breathing human to increase the signal-to-noise ratio of the measurements. The aerosol particles are released into the room using a generic face – also known from first aid courses – which is mounted in the breathing zone of the surgeon, see Fig. 4, for cases 1 and 2. Please note that the spreading of larger particles which might be produced during, e.g., coughing, sneezing or talking, is not investigated in the present study as these particles are filtered by the surgical masks very effectively and thus should not be released in high concentrations in an operation room.

2.2.2 Aerosol Detection

For the acquisition of the local aerosol concentrations at many positions in the operation room, the mobile measurement system of the DLR was applied [15, 16]. Low-cost particulate matter sensors (Sensirion SPS30) are used, ensuring an accuracy of $20\ \#/\text{cm}^3$ or 10% of the measured value (whatever is larger). The data acquisition is performed using a sensor grid of more than 50 particulate matter sensors at approximately 1 Hz measurement frequency allowing for a reasonable resolution in space and time. The sensors were mainly installed at three different heights, i.e., 1.20 m, 1.70 m and 2.20 m above the floor, with 14 sensors per height, see green stars in Fig. 3. The six inner positions correspond to the operation table ‘TAB’, the next four positions to the circle around the table ‘CIR’ and the four outer positions to the vicinity ‘VIC’. At the positions ‘CIR’ and ‘VIC’ additional sensors are installed at a height of 0.45 m. Furthermore, two sensors are installed next to the exhaust air openings, see blue stars in Fig. 3, at a height of 0.25 m.

The background concentration of aerosol particles in the operation room was below the lower detection limit of the applied measurement systems confirming the proper installation and function of the HEPA filters in the supply air system.

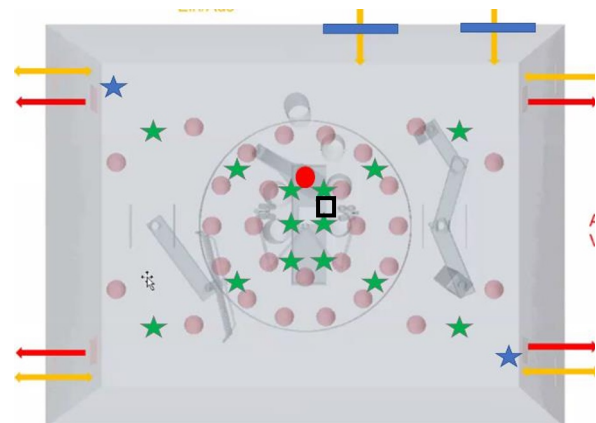


Fig. 3. Sketch of the Particulate Matter Sensors in one selected measurement plane. The green stars mark the positions of the sensors attached to the tripods. The blue stars mark the additional sensors next to two of the exhaust air openings. The blue bars in the top right corner represent the two doors of the operation room. The red dot marks the position of the head of the patient and the black square represents the position of the aerosol source, for cases 1 and 2 in the exhalation zone of the surgeon and for case 3 below the ceiling.

2.3 Investigated Cases and Configurations

The investigated cases can be divided into two main categories: Firstly, particles are released through the exhalation of a member of staff in the room which might potentially settle in the operation wound, see Fig. 4. Secondly, the aerosol particles are released in the ceiling area above and slightly next to the position of the standing surgeon. While the first case represents a

realistic aerosol source location, the second case is chosen to increase the knowledge on the air low pattern in the room and to evaluate the impact of movement, i.e., dynamic situations on this general airflow pattern. Three different test cases are presented in this paper and summarized in Tab. 1. The dynamic case 3 comprises a typical configuration during an operation. Firstly, a member of staff leaves the operation room to get some additional surgery instruments or other equipment ($t = 300$ s). Five minutes later, the person re-enters the operation room ($t = 600$ s), walks to the assistant at the operation table and hands over the box with the additional instruments ($t = 640$ s). At $t = 900$ s, the surgeon starts to use the instruments and operates on the patient for five minutes. Afterwards, the surgeon stops and removes the instruments ($t = 1200$ s). The other two test cases are static configurations with (case 2) and without (case 1) the hands of the surgeon at the instruments. The aerosol exhalation is simulated in the breathing zone of the surgeon for these cases, see Fig. 4.

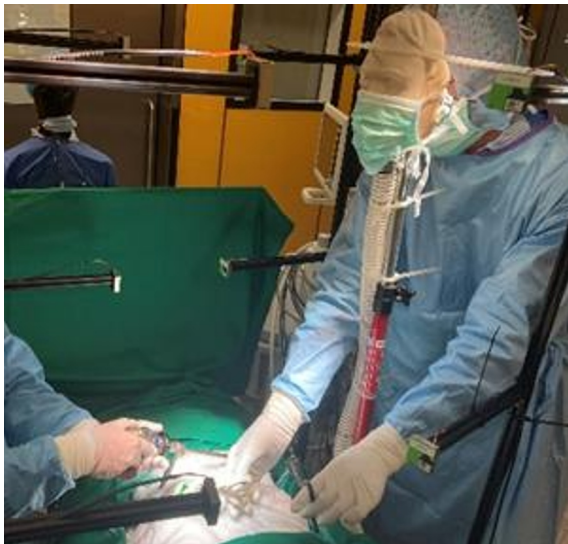


Fig. 4. Aerosol exhalation for standing staff and local aerosol concentration probes above the patient. (case 2)

Tab. 1: Summary of test cases.

	Source	Remarks
Case 1 (ID42)	Surgeon	Static No use of instruments
Case 2 (ID43)	Surgeon	Static With hands on instruments
Case 3 (ID41)	Ceiling	Dynamic case $t = 0$ s: start of aerosol source $t = 300$ s: open door, person leaves OR (1) $t = 600$ s: open door, person enters OR (2), brings box to assistant (arrives at $t=640$ s) $t = 900$ s: surgeon uses instruments in the abdomen of the patient (3) $t = 1200$ s: surgeon stops and removes instruments (4) $t = 1500$ s: stop of aerosol source

3 Results

First, we will discuss the stationary case with the aerosol source in the breathing zone of the surgeon. After having exemplarily shown concentration-time curves of selected measurement positions, we will compare the spreading behavior of the particles for the cases 1 and 2, i.e., with and without the hands and arms using the surgery instruments above the patient.

In the second sub-section, we will evaluate the dynamic case 3, where the door is opened twice, a person walks through the room and the surgeon works for 5 minutes with the above the patient using the surgery instruments.

3.1 Source at Surgeon

First results showed that the aerosol particles exhaled by the standing source are down-washed by the airflow and reach, strongly diluted, one of the sensor positions above the operation table next to the standing source, see Fig. 5 (top). Local concentrations as low as $\approx 1.5\%$ of the exhalation concentration (c.f. $N \approx 3000 \text{ \#/cm}^3$) are found. All other positions above the operation table show a particle concentration close to zero. With a certain time delay the cloud of exhaled aerosol particles reaches single other sensor locations on its way towards the exhaust openings, see Fig 5 (bottom), while being further diluted, $\approx 0.03\%$ of the exhalation concentration (c.f. $N \approx 60 \text{ \#/cm}^3$).

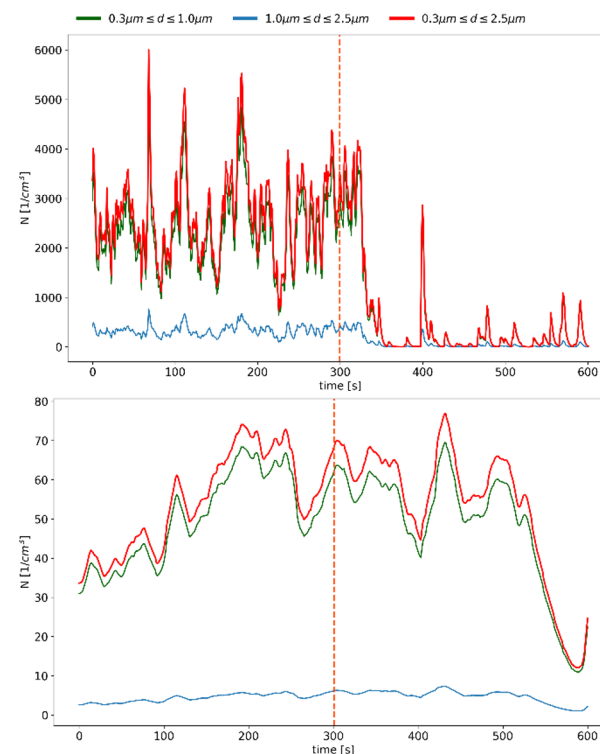


Fig. 5. Exemplary concentration-time curves at selected measurement positions above the table in the downwash area of the exhaled particles (top) and at 1.20 m height in the vicinity (bottom) (stationary case 2). The aerosol source was stopped at $t = 300$ s. Note: different y-scales are used.

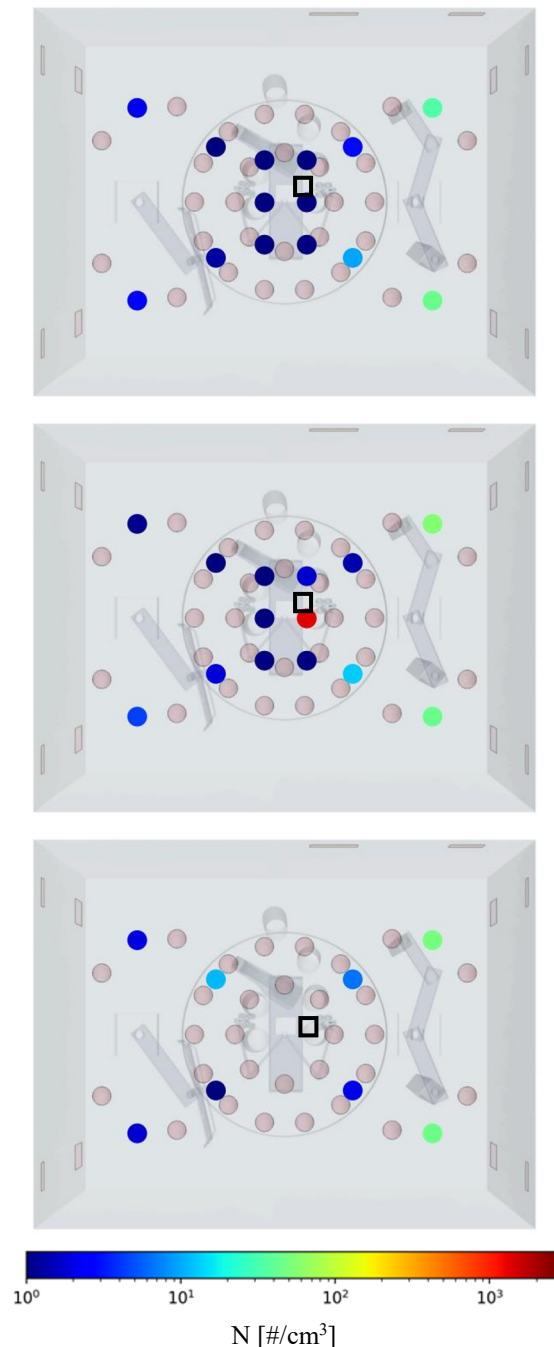


Fig. 6. Spatial spreading of the aerosol particles for case 1 (no use of surgery instruments) recorded at three different heights: top: 1.70 m; middle: 1.20 m and bottom: 0.45 m above the floor. The black square represents the position of the aerosol source below the ceiling.

Figure 6 presents the spatial distribution of the time-averaged local aerosol concentrations at three different heights: 1.70 m (top), 1.20 m (middle) and 0.45 m (bottom) for the case 1, i.e., the aerosol source in the breathing zone of the surgeon and without the use of instruments. The highest particle concentration was found for the intermediate height directly above the table and directly below the exhalation zone of the surgeon. Accordingly, in the region directly above the operation table, i.e., below the majority of the ceiling air supply openings, the forced downwash of the air outbalances the thermal plume induced by the heat

release of the persons. In the higher measurement plane (Fig. 6, top), we only recorded values which are approximately a factor of 30 lower than the highest value. However, in this plane, at 1.70 m, some particles were detected in the vicinity (VIC) in the right half of the operation room, i.e., on the side where the surgeon was standing. A similar pattern, but with slightly higher values was also detected above the floor on the 0.45 m measurement plane, see Fig. 6 (bottom).

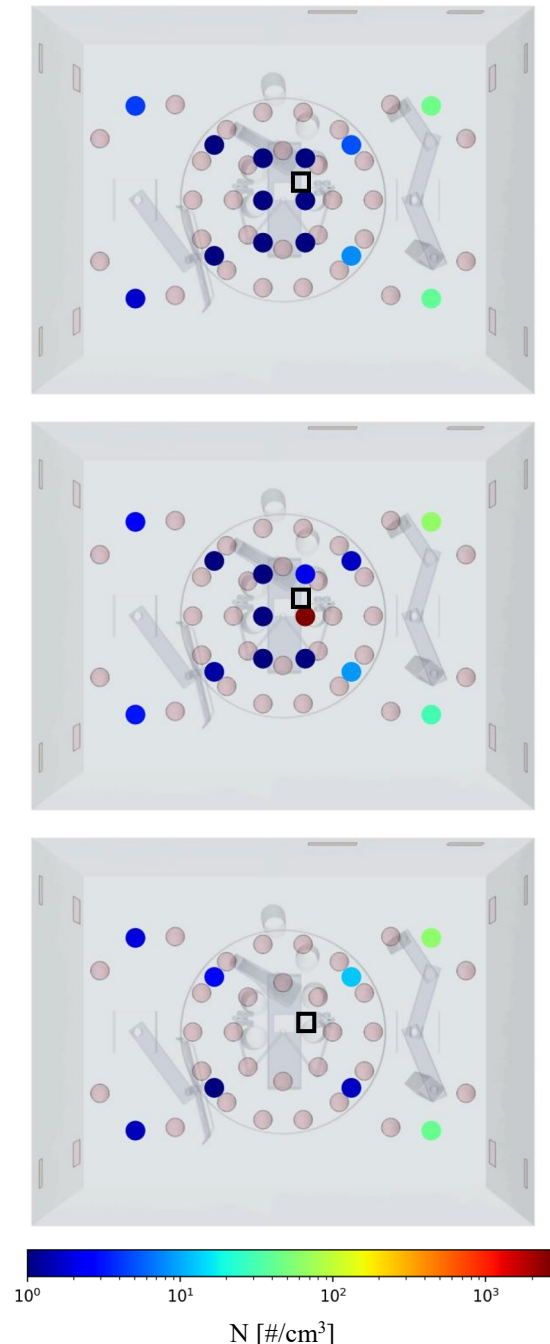


Fig. 7. Spatial spreading of the aerosol particles for case 2 (with hands using the surgery instruments) recorded at three different heights: top: 1.70 m; middle: 1.20 m and bottom: 0.45 m above the floor. The black square represents the position of the aerosol source below the ceiling.

Figure 7 presents the same evaluation as Figure 6, but for the case with the hands of the surgeon using the instruments above the patient, c.f. case 2. Again, the highest local particle concentration was found at table height directly below the exhalation region of the surgeon. The rest of the aerosol particle distribution in the room at the other heights is also very similar to case 1. Accordingly, we can conclude that the different positions of the hands and arms of the surgeon and his/her instruments do not change the overall flow pattern in the operation room.

However, case 2 revealed much higher local concentrations compared to case 1. Above the table, values were recorded, which were approximately a factor of two higher. As a result, we summarize that locally strong changes of the particle concentrations occur, especially in the direct region of the downwash of the exhaled air with high particle concentrations.

3.2 Dynamic Case: Source at Ceiling

Figure 8 shows the time-concentration curves for four selected measurement positions during the dynamic case. Additional vertical black dash-dotted lines are included representing the moment (1) the door was opened for the first time and the staff person leaves the operation room ($t = 300$ s); (2) the door was opened the second time and the person re-entered the operation room with a box which is then carried to the assistant at the operation table ($t = 600$ s); (3) the surgeon started to work with the instruments above the patient ($t = 900$ s); and (4) the moment the surgeon stopped working with the instruments ($t = 1200$ s). The last red vertical line indicates the time the aerosol generator was stopped. The four measurement positions are at floor level in the lower right circle (a) and at three different positions on the table at a height of 1.20 m. Here (b) was at the lower end of the operation table on the side of the surgeon, (c) in the central part of the table on the side of the surgeon and (d) on the opposite side of (c). At this point it should be noted that all other particle sensors in the room did not show significant changes during this measurement run.

The first thing to note is that the initial opening of the door at $t = 300$ s as well as the second door opening at $t = 600$ s do not have a significant influence on the local particle concentrations. However, shortly after the second door opening corresponding to the time, when the staff arrives at the operation table at $t = 640$ s (see also Tab. 1) we observe a short but strong increase of the local particle concentration at the sensor at floor level from zero to more than 200 #/cm^3 , see Fig. 8 (a). This peak can be attributed to a transient flow field, e.g., in the wake region of the moving staff, which transports the particles to the sensor position. Simultaneously, we observe a small yet visible change of the aerosol particle concentrations in the central part of the operation table, see Fig. 8 (c) and (d). This indicates that the airflow above the table is also weakly influenced by the moving person and the transport box being handed over to the assistant next to the operation table.

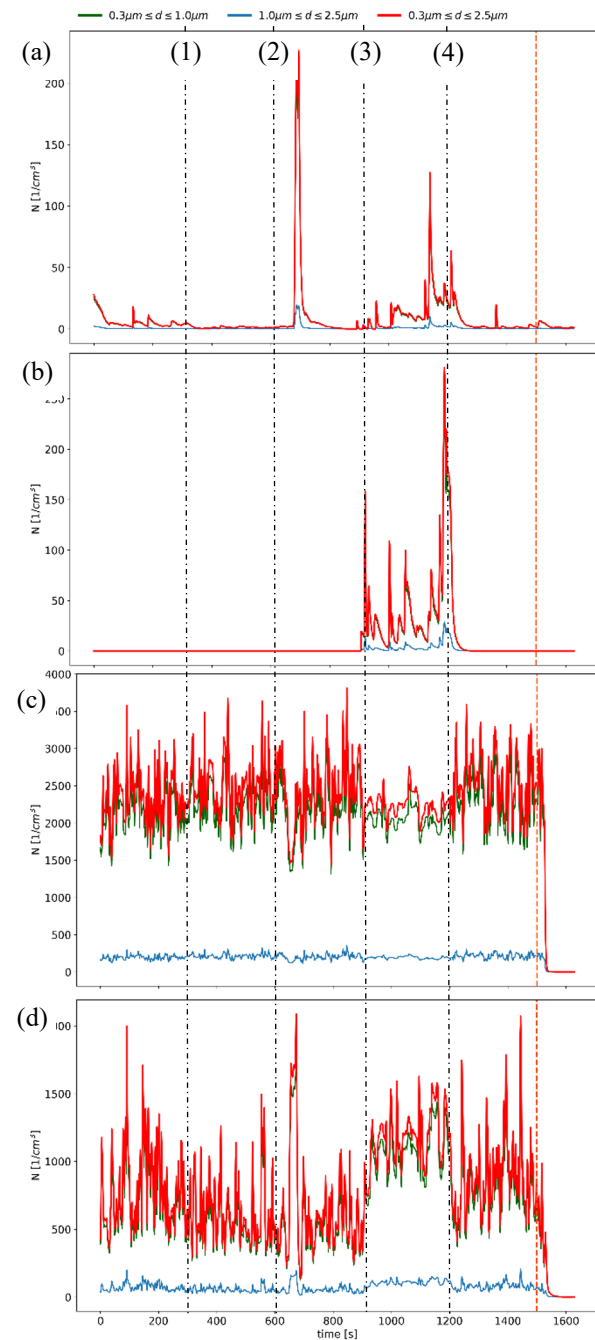


Fig. 8. Local aerosol particle concentrations at for selected positions for the dynamic case 3. (a) CIR4-045, (b) TAB6-120, (c) TAB2-120, (d) TAB5-120. Note: different y-scales are used. Activities at (1) to (4), see Tab. 1.

The most significant change, observed at all four measurement positions, is found for the time period in which the surgeon is using the surgery instruments above the patient, i.e., $t = 900$ s to $t = 1200$ s. During the activity, that is, while the surgeon is performing operation-like movements with the surgery instruments above the patient, a strong change of the local aerosol concentrations above the operation table can be observed. Here, the airflow with the aerosol particles is deflected by the movement and the additional obstructions above the patient resulting in decreased values directly below the original downwash, see Fig. 8 (c). Simultaneously, the local concentration increases at

the opposite side of the operation table (d) and reaches regions, which had not been affected by the particles before at (b).

The findings highlight the effect of dynamic situations, i.e., motion of the surgeon and the staff in the operation room on the local aerosol particle spreading. Furthermore, the data will help to establish a data base for the validation of computational fluid dynamics simulations of the airflow at such dynamic configurations.

4 Conclusions and Outlook

This paper presents an experimental investigation of aerosol particle spreading in an operation room. Different configurations regarding the source position or representative movements of the staff in the room are analyzed.

Firstly, we found that the position of the surgeon, i.e., with or without the hands using the surgery instruments above the patient, does not change the overall distribution of the particles exhaled in the breathing zone of the surgeon. However, especially on the operation table, the local particle concentrations change by a factor of about two. This finding implies that a precise knowledge the transport paths of exhaled or otherwise generated aerosol particles will help to reduce possible cross contaminations. In specific, blocking the transport paths, e.g., by moving the arms, changes the local particle concentrations in potentially critical areas. Please note that this change might be positive or negative depending on the air flow pattern the relative positions of the particle source and the critical area.

During the dynamic case representing a typical situation in an operation room, we found neglectable effects during door openings, a weak effect caused by the movement of the staff through the room and a strong effect on the aerosol concentration above the operation table during the time when the surgeon is working with the surgery instruments above the patient.

The findings highlight the importance that only conscious movements are carried out in an operation room. Furthermore, the obtained data will help to enhance and validate numerical simulation models which include the dynamic movement in such a room.

In future studies, both experimentally and numerically, the air flow pattern and the connected transmission paths of exhaled aerosol particles should be analyzed in various healthcare facilities. The identification and enhanced knowledge of the airborne transmission routes, especially in rooms with guided air flows, will help to even further reduce the risk of cross infections.

Acknowledgements and Funding



vis

The authors are thankful to the whole team of the c3vis project from OHB, Merkle & Partner, OTH Amberg-Weiden and University Medicine Leipzig for their support during the measurements.

Further, the authors would like to thank Annika Köhne for proof-reading the manuscript.

This work was partially supported by the c3vis project, coordinated by OHB and funded by DLR-ESA Spark funding and partially supported by the Initiative and Networking Fund of the Helmholtz Association of German Research Centres (HGF) under the CORAERO project (KA1-Co-06).



References

1. S. Sadrizadeh et al. (19 co-authors), “A systematic review of operating room ventilation”, J. Build. Engineering 40, p.102693, 2021. doi: 10.1016/j.jobe.2021.102693
2. M.D.A. Melhado, J.L.M. Hensen, M.G.L.C. Loomans, (2006). Review of operating room ventilation standards. Proceedings of the 17th Int. Air-conditioning and Ventilation Conference. Prague: STP - Society of Environmental Engineering.
3. Z. Liu, H. Liu, H. Yin, R. Rong, G. Cao, Q. Deng, “Prevention of surgical site infection under different ventilation systems in operating room environment”, Front. Environ. Sci. Eng. 15, 36, 2021. doi: 10.1007/s11783-020-1327-9
4. B. Surial, A. Atkinson, R. Külpmann, A. Brunner, K. Hildebrand, B. Sicre, N. Troillet, A. Widmer, E. Rolli, J. Maag, J. Marschall : “Better Operating Room Ventilation as Determined by a Novel Ventilation Index is Associated With Lower Rates of Surgical Site Infections“. Annals of Surgery, 276(5):e353-e360, 2022. doi: 10.1097/SLA.0000000000005670
5. C. Wang, S. Holmberg, S. Sadrizadeh, “Numerical study of temperature-controlled airflow in comparison with turbulent mixing and laminar airflow for operating room ventilation”, Building and Environment 114, 45-56, 2018. doi: 10.1016/j.buildenv.2018.08.010
6. K. Xue, G. Cao, M. Liu, Y. Zhang, C. Pedersen, H.M. Mathisen, L.-I. Stenstad, J.G. Skogås : “Experimental study on the effect of exhaust airflows on the surgical environment in an operating room with mixing ventilation“, Journal of Building Engineering, 32,101837, 2020, doi : 10.1016/j.jobe.2020.101837.
7. W.A.C. Zoon, M.G.L.C. Loomans, J.L.M. Hensen, “Testing the effectiveness of operating room ventilation with regard to removal of bacteria”, Building and Environment, 46, 2570-2577, 2011. doi: 10.1016/j.buildenv.2011.06.015
8. R. Wood: “Experimental and theoretical studies of contaminant transport due to human movement in a hospital corridor“. PhD thesis, University of Leeds, UK (2015).
9. T.-T. Chow, J. Wang : “Dynamic simulation on impact of surgeon bending movement on bacteria-

- carrying particles distribution in operating theatre“, *Building and Environment*, **57**, 68-80, 2012. doi :10.1016/j.buildenv.2012.04.010.
10. <https://www.oth-aw.de/bulitta/lehr-und-forschungs-op/> (accessed, 20th July 2023), see sketches and video animation of operation room
 11. S. Buhl, N. Eschenbecher, C. Bulitta: “Erste Ergebnisse und Erfahrungen mit einem neuartigen OP-Lüftungskonzept auf Basis einer temperaturkontrollierten Luftströmung“, (in German) *Krankenhaus-Hygiene + Infektionsverhütung*, **38**, 67-73, 2016. doi : 10.1016/j.khinf.2015.12.004.
 12. C. Bulitta, F. Magerl, R. Hartwich, B. Russwurm: “CFD analysis of a high-tech operating room using Star-CCM+“. In: Magazine DYNAMICS from CD-adapco / Issue 38, pages 22 to 25, 2015.
 13. D. Schmeling, A. Shishkin, D. Schiepel, C. Wagner: “Numerical and experimental study of aerosol dispersion in the Do728 aircraft cabin“. *CEAS Aeronautical Journal* **14**, 509-526 (2023). doi: 10.1007/s13272-023-00644-3.
 14. D. Schmeling, M. Kühn, D. Schiepel, A. Dannhauer, P. Lange, A. Kohl, K. Niehaus, T. Berlitz, M. Jäckle, T. Kwitschinski, T. Tielkes: “Analysis of aerosol spreading in a German Inter City Express (ICE) train carriage“. *Building and Environment* **222**, 109363 (2022). doi: 10.1016/j.buildenv.2022.109363.
 15. K. Niehaus and A. Westhoff, “An open-source data acquisition system for laboratory and industrial scale applications,” *Meas. Sci. Technol.*, vol. 34, p. 027001, 2022. doi: 10.1088/1361-6501/ac9994
 16. K. Niehaus, “Mobile measurement system,” 2022. doi:10.5281/zenodo.6471388